

Small Satellite Space Environments Effects Test Facility

JR Dennison,¹ Kent Hartley,^{1,2} Lisa Phillipps,^{1,2} Justin Dekany,¹ and Robert H. Johnson,^{1,2,3}
 Physics Department, Logan, UT 84322-4415 USA; (435) 797-2936

JR.Dennison@USU.edu

James S. Dyer

Space Dynamics Laboratory, Utah State University
 North Logan, UT 84341 USA; (435) 713-3545

Jim.Dyer@SDL.USU.edu

¹ Materials Physics Group, Physics Department, Utah State University

² Mechanical Engineering Department, Utah State University

³ Kern River Gas Transmission Company

ABSTRACT

A versatile test facility has been designed and built to study space environments effects on small satellites and system components. Testing for potentially environmental-induced modifications of small satellites is critical to avoid possible deleterious or catastrophic effects over the duration of space mission. This is increasingly more important as small satellite programs have longer mission lifetimes, expand to more harsh environments (such as polar or geosynchronous orbits), make more diverse and sensitive measurements, minimize shielding to reduce mass, and utilize more compact and sensitive electronics (often including untested off-the-shelf components). The vacuum chamber described here is particularly well suited for cost-effective, long-duration tests of modifications due to exposure to simulated space environment conditions for CubeSats, system components, and small scale materials samples of >10 cm X 10 cm. The facility simulates critical environmental components including the neutral gas atmosphere, the FUV/UV/VIS/NIR solar spectrum, electron plasma fluxes, and temperature. The solar spectrum (~120 nm to 2500 nm) is simulated using an Solar Simulator and Kr resonance lamps at up to four Suns intensity. Low and intermediate electron flood guns and a Sr⁹⁰ β radiation source provide uniform, stable, electron flux (~20 eV to 2.5 MeV) over the CubeSat surface at >5X intensities of the geosynchronous spectrum. Stable temperatures from 100 K to 450 K are possible. An automated data acquisition system periodically monitors and records the environmental conditions, sample photographs, UV/VIS/NIR reflectivity, IR absorptivity/emissivity, and surface voltage over the CubeSat face and *in situ* calibration standards during the sample exposure cycle.

INTRODUCTION

To paraphrase Douglas Adams,¹ “Space is [harsh]. You just won’t believe how vastly, hugely, mind-bogglingly [harsh] it is.” Interactions with this harsh space environment can modify materials and cause unforeseen and detrimental effects to spacecrafts.^{2,3} If these are severe enough the spacecraft will not operate as designed or in extreme case may fail altogether.^{2,4} Environmentally-induced problems are dominated by spacecraft charging^{3,5,6} and single-event interrupts.^{2,10} Exposure to higher fluence radiation UV^{7,8} and radiation^{7,9,10} can generate atomic scale defects in materials leading to changes in the optical, electrical, and mechanical properties. Alternately, temperature fluctuation,¹¹ charged particle flux,¹² contamination,^{13,14} or surface modifications^{15,16} can lead to materials modifications and changes in optical, thermal, and charging properties of the materials.¹⁷ The evolution of the charging, discharging, electron transport, and arcing

properties of surface and bulk materials as a result of prolonged exposure to the space environment has been identified as one of the critical areas of research in spacecraft charging.¹⁸ Further, materials modifications can change the satellite environment, leading to feedback mechanisms for further spacecraft responses.¹⁷

Testing for potentially environmental-induced modifications of small satellites is critical to avoid possible deleterious or catastrophic effects over the duration their missions. Small satellites are particularly susceptible to such problems, as they usually have minimal shielding to meet reduced mass and size constraints^{19,20} and often utilize more compact and sensitive electronics (often including untested off-the-shelf components).^{20,21} This is increasingly more important as small satellite programs have longer mission lifetimes and make more diverse and sensitive

measurements.²⁰ The current push to expand deployment of CubeSats beyond LEO²² and into even more demanding environments where modest relief due to shielding by the Earth's magnetosphere is absent (such as polar or geosynchronous orbits) can further exacerbate these problems.^{2,23}

The key to predicting and mitigating these harmful effects is to develop a broad knowledgebase of the changes produced in the very broad range of materials in spacecraft applications under a wide range of environmental conditions and how these changes affect the materials properties critical to space operations.^{7,24-27} This necessitates the ability to accurately simulate space environment effects through long-duration, well-characterized testing in an accelerated, flexible laboratory environment.²⁸⁻³²

Such is the motivation for developing the versatile, modular Space Survivability Test (SST) facility described here, designed to study these effects on small satellites and system components. The SST vacuum chamber is particularly well suited for cost-effective, long-duration tests of modifications due to exposure to simulated space environment conditions for CubeSats, system components, and small scale materials samples. The design criteria and instrumentation details of the chamber are described below.

SPACE SIMULATION CAPABILITIES

There are a number of characteristics that are necessary for a realistic simulation of different space environments. Many of these critical characteristics are simulated in the SST chamber, including vacuum and neutral gas environment [high vacuum (10^{-7} Pa) to ambient], temperature (100 K to 450 K), the FUV/UV/VIS/NIR electromagnetic solar spectrum (120 nm to 2000 nm), electron plasma fluxes (10^1 eV to 10^6 eV), and radiation effects. Other characteristics, not yet simulated in the SST chamber, include low temperature plasmas, proton or ion flux, and atomic oxygen flux.

The neutral gas environment composition and pressure varies substantially in different near-Earth environments and can be dominated by local outgassing from spacecraft.² For low-earth orbit (LEO) environments most common for CubeSats, composition is dominated (in decreasing order) by O, N₂, O₂, H, He, and Ar.^{2,20} The vacuum of space in LEO is typically $<10^{-7}$ Pa, but can be $>10^{-3}$ Pa in local space environments due to outgassing or mass ejection. Pressure variations have significant impact on material outgassing, contamination rates, susceptibility to arcing, and thermal transport.

Spacecraft are typically designed with an operational temperature range from 200 K to 350 K in near-earth orbits, depending on exposure to the solar spectrum and the reflectivity and emissivity of materials.² However, they can extend to higher or lower temperatures in orbits far from Earth or when purposefully shielded from solar radiation.² Temperature control can be particularly challenging for satellites, such as CubeSats, with smaller radiating areas.^{20,21} Mechanical and electrical properties of materials are particularly susceptible to temperature changes.

The electromagnetic solar spectrum (see Figure 1(a)) is dominated by blackbody radiation from the sun peaked in the visible; the vast majority of incident power is from UV/VIS/NIR radiation from ~ 250 nm to ~ 5000 nm that results in most material heating. Photo-excitation, ionization and defect generation, however, more often result from higher energy (≥ 5 eV or ≤ 250 nm) incident radiation. The power in the spectral region <250 nm has its strongest component from the hydrogen Lyman- α emission line at 121.6 nm (see Figure 1(a)). The Lyman- α emission can dominate many important materials properties; e.g., Ly- α emission is responsible for between 15% and 85% of photoemission from typical spacecraft materials.³³⁻³⁶ UV materials degradation and radiant heating are the most common problem for CubeSats in LEO orbits,^{19,21} though charging from photoemission can be important in other near-earth orbits.^{1,33}

The electron flux for near-earth orbits can vary dramatically,^{2,40-42} as shown in Figure 1(b). The majority of spacecraft anomalies attributed to the space environment are spacecraft charging effects.⁵ Electrons with energies ≤ 30 keV are responsible for most surface charging effects.^{2,37} The higher pressures in LEO reduce the importance of surface charging for CubeSats in LEO.^{20,21} Even though fluxes of higher energy electrons are reduced by orders of magnitude, they are largely responsible for significant environment-induced effects such as deep dielectric charging,^{23,38} single event interrupts,^{2,10,20} and radiation damage.^{9,10,38} These effects from high energy electrons (and protons) have been identified as serious potential threats for CubeSats in all near-earth orbits.¹⁹ This is exacerbated for CubeSats because of the reduction in shielding necessitated by size and mass constraints of small satellites. For example, if fully 10% (~ 0.1 kg) of a CubeSat's mass were devoted to a ~ 1 mm thick Al shield over all CubeSat faces, this shield would be insufficient to stop electrons with ≥ 300 keV.

EXPERIMENTAL TEST CHAMBER DESIGN

A versatile ultrahigh vacuum test chamber has been designed for long duration testing of materials

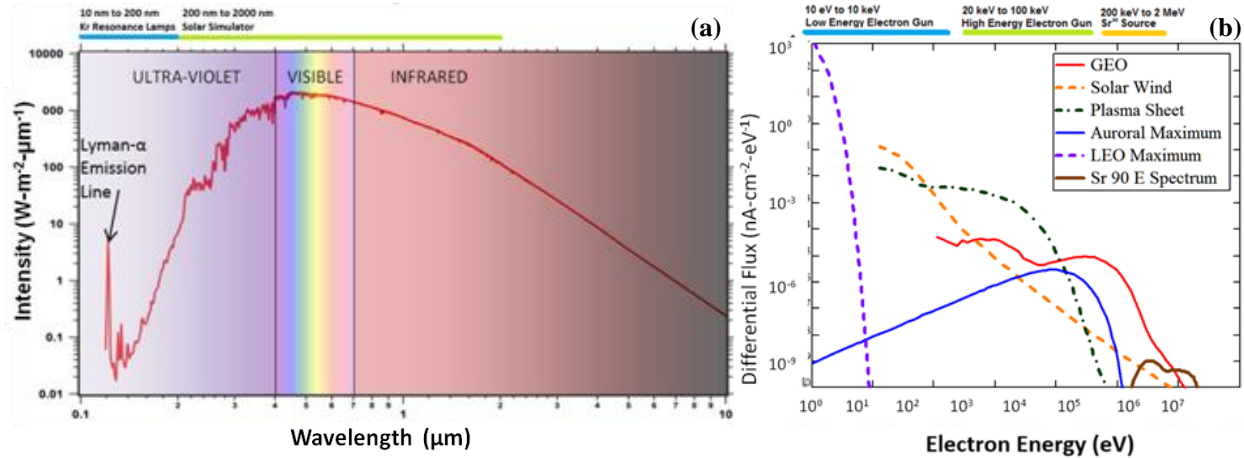


Figure 1. (a) AM0 solar electromagnetic spectrum.⁴⁰ (b) Representative space electron flux spectra for geostationary earth orbit,² solar wind at the mean earth orbital distance,⁴¹ plasma sheet environment,⁴¹ maximum aurora environment,⁴² and low earth orbit.² The Sr⁹⁰ source emission spectrum is also shown. Bars above graphs show the ranges of the chamber source emissions.

modifications due to exposure to simulated space environment conditions (see Figure 2). It provides a controlled temperature and vacuum environment with stable, uniform, long-duration photon and electron fluxes at up to 4 times GEO equivalent intensities for accelerated testing for a sample area of ≥ 10 cm by 10 cm. The full FUV/UV/VIS/NIR spectrum of photon energies with appreciable intensities in the space environment is simulated. Two separate monoenergetic electron sources and a broadband high energy electron source are used to simulate electron fluxes over most of the energy range with appreciable electron intensities. The simultaneous use of multiple source allows a reasonable simulation of synergistic broad band energy fluxes encountered in typical space environments; combinations of simultaneous low and high energy electron beams³⁹ and simultaneous photon and electron beams³⁶ have been found to be important under certain circumstances.

The chamber maintains $\geq 95\%$ uniformity of the EMS and electron radiation exposure over the full sample area (see Figure 3). The long-term exposure variability of individual samples can be further reduced by periodically rotating the sample stage. The footprint of the incident radiation on the sample surface (see Figure 2(a)) is determined by a flux mask (**E**; see the legend of Figure 2 for definitions of these letters) located near the chamber's top ports that restricts the flux boundaries to the sample stage, limiting equipment exposure and reducing scattering to accommodate uniform exposure. The solar simulator flux is collimated, but the FUV and electron beams diverge as point sources recessed outside the main vacuum chamber, as shown in Figure

2(a). Additional viewports allow for visual inspection of the samples and flux sources during the sample exposure cycle.

Sample Accommodation

Three versatile custom rotatable sample test fixtures are shown in Figure 2 for evaluation of: (i) materials, (ii) Cubesats, and (iii) COTS electronics and custom circuits. These test fixtures and the chamber radiation mask allow for cost-effective, customizable investigations of multiple small-scale samples.

Material samples mounted on a temperature-controlled rotating carousel (Fig. 1(d)) can be readily reconfigured for one 10 cm diameter sample or multiple smaller samples. The OFHC Cu sample carousel (**M**) connected to a standard rotary vacuum feedthrough (**S**), used for 355° rotation to position samples under the probe translation stage (**T**) and to enhance flux uniformity by periodic rotation. The sample stage shown in Figure 2(e) has six 2.5 cm diameter samples (**L**), plus four flux sensors (**I,J**) and platinum resistance temperature probes (**K**). *In-flux* environmental monitoring and *in-situ* sample characterization capabilities allow characterization at frequent intervals during an exposure cycle, while samples are still under vacuum. A similar fixture (Fig. 1(f)) allows exposure of a CubeSat face, with sufficient wiring capabilities for *in-flux* testing of on-board systems and electronics. A third fixture (Fig. 1(g)) includes a custom radiation hardened prototyping breadboard and PC board mounting, with extensive vacuum feedthrough wiring capacity for *in-flux* and *in situ* monitoring of environment- and radiation-induced failures of custom circuits and COTS parts.

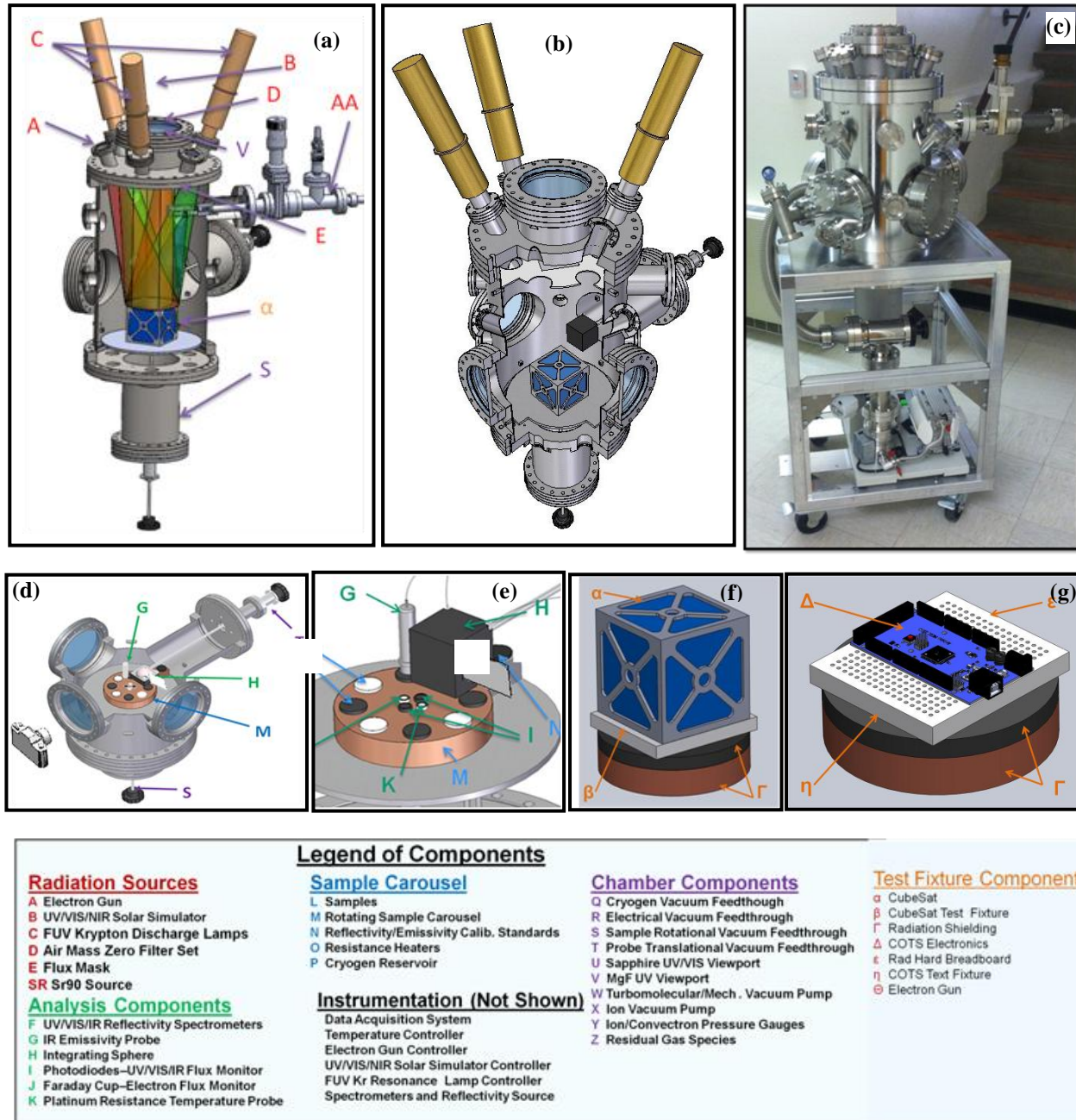


Figure 2. Space Survivability Test (SST) chamber. (a) Cutaway view of beam trajectories, with materials sample carousel. (i) UVA/VIS/NIR light (yellow). (ii) UVF light (green). (iii) Intermediate-energy (<100 keV) electron beam (red). Low-energy (<5 keV) electron beam (orange). (iv) (v) Sr⁹⁰ beta radiation (<2.2 MeV) beam (blue). (b) Chamber vertical cutaway view, with CubeSat test fixture. (c) Exterior view of assembled chamber. (d) View of sample carousel stage and characterization probes for materials tests. (e) Materials test fixture. (f) CubeSat test fixture. (g) COTS test fixture.

These interchangeable test fixtures work with the main SST chamber, as well as in other configurations with several existing test chambers (e.g., USU Electron Emission Test chamber³² and the USU pulsed electro-acoustic embedded charge distribution test chamber⁴³). Alternately, the SST chamber can also be reconfigured

as a radiation source for other test chambers by removing the same sample stage flange and bolting the upper source components to other test chambers using the lower 36 cm flange (see Figure 4(c)). For example, the modular design allows the sources to mate separately with a larger SDL Ion Optics Test chamber

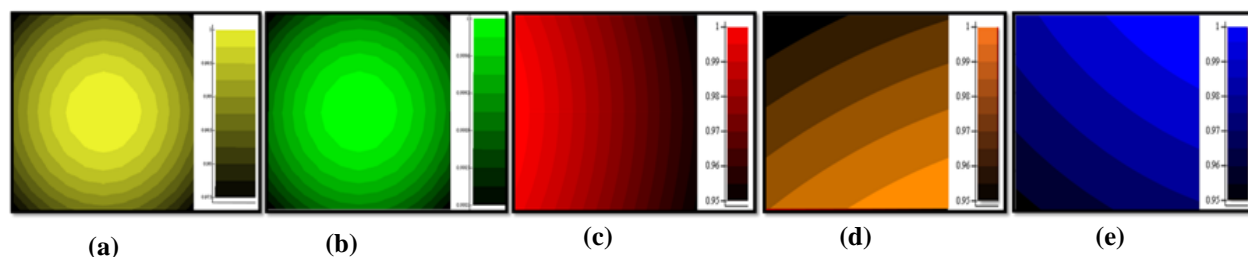


Fig. 3. Contour plots of exposure intensity on 10 cm X 10 cm CubeSat face: (a) UVA/VIS/NIR light. (b) UVF light. (c) High Energy Electron Beam. (d) Low Energy Electron Beam. (e) Sr⁹⁰ Radiation. Variation in relative intensity shown by the color scales at right do not exceed ±3%.

with an ion gun and beam diagnostics which can emulate ion drift measurement environments; this chamber has a 5-axis rotation/ translation manipulator that can position the faces of a CubeSat (up to 3U) relative to all incident beams. These alternate configurations are illustrated in Figure 4.

Vacuum and Neutral Gas Environment

The vacuum chamber uses standard mechanical and turbomolecular pumps (X) for roughing and an ion pump (Y) for continuous maintenance-free high vacuum operation. Standard UHV ConflatTM flanges, feedthroughs, and valves are used. Neutral gas density and composition can be regulated from the base pressure (high vacuum <10⁻⁵ Pa) to ambient using an ultrahigh vacuum leak valve and gas handling system. Pressure is monitored with ConvectronTM, ion gauges (Y) and a residual gas analyzer (Z).

Temperature

A stable, controlled, uniform temperature range from ~100 K to 450 K is maintained to ±2 K by a standard PID temperature controller, using a cryogenic reservoir (P) and resistance heaters (O) attached to a large thermal mass sample stage (M) used to minimize the differences in temperature between samples and thermal fluctuations during the sample exposure cycle. Fluids circulated through the reservoir from a temperature calibration bath are used for the range 260 K to 360 K; liquid nitrogen is used from ~100 K to ~250 K.

Alternately, sample temperatures from ~30 K to 350 K can be achieved using a closed-cycle helium cryostat (Air Products, Displex DE-202-0-SP) and a different sample stage (see Figure 4(a)) bolted to the flange where the sample stage rotational vacuum feedthrough (S) is fastened. Temperatures can be maintained to within <0.5 K by a standard PID temperature controller using platinum resistance sensors. Details of this sample stage are provided by Dekany.⁴⁴

UV/VIS/NIR Solar Spectrum Photon Fluxes

The UV/VIS/NIR solar spectrum is simulated over the full spectrum of photon energies with appreciable intensities in the space environment using a solar simulator and Kr resonance lamps. An external, normally incidence and collimated commercial class AAA solar simulator source (B) (Photo Emission Tech, Model SS80AAA) provides >98% flux uniformity (Figure 3(a)). It uses a Xe discharge tube, parabolic reflector, and collimating lens with standard Air Mass Zero (AM0) filters (Photo Emission Tech) (D) to shape the incident radiation spectrum to match the NIR/VIS/UVA/UVB solar spectrum (from 200 nm to 1700 nm) at up to 4 times sun equivalent intensity for accelerated testing over an area of >10 cm X 10 cm. Additional filters for AM1 and AM1.5 spectra and a bandpass filter to minimize sample heating by blocking the IR spectral components are also available. Light intensity feedback is used to maintain the intensity temporal stability to within <2% during the sample exposure cycle, using standard calibrated solar photodiodes mounted internally on the sample mounting block. Solar simulator normally incident UV/VIS/NIR light passes through a sapphire viewport (U). Xe bulbs have >1 month lifetimes and are readily replaced *ex situ* for long duration studies.

Incident FUV (far ultraviolet) solar radiation is simulated by Kr discharge resonance line sources (Resonance Limited, Model KrLM-L) (C), with a primary emission lines at 124 nm and secondary emission line at 117 nm, with up to 4 times sun equivalent intensity. This provides an adequate substitution for the solar vacuum ultraviolet spectrum (~200 nm to ~10 nm), which is dominated by the H Lyman- α emission line at 122 nm. Three lamps oriented 120° apart provide >98% flux uniformity (Figure 3(b)). The Kr source computer automation system allows monitoring and up to 1 kHz modulation of the output intensity, plus closed-loop temperature control of the source heater and RF output. Kr bulbs have ~5 month lifetimes for long duration studies; they

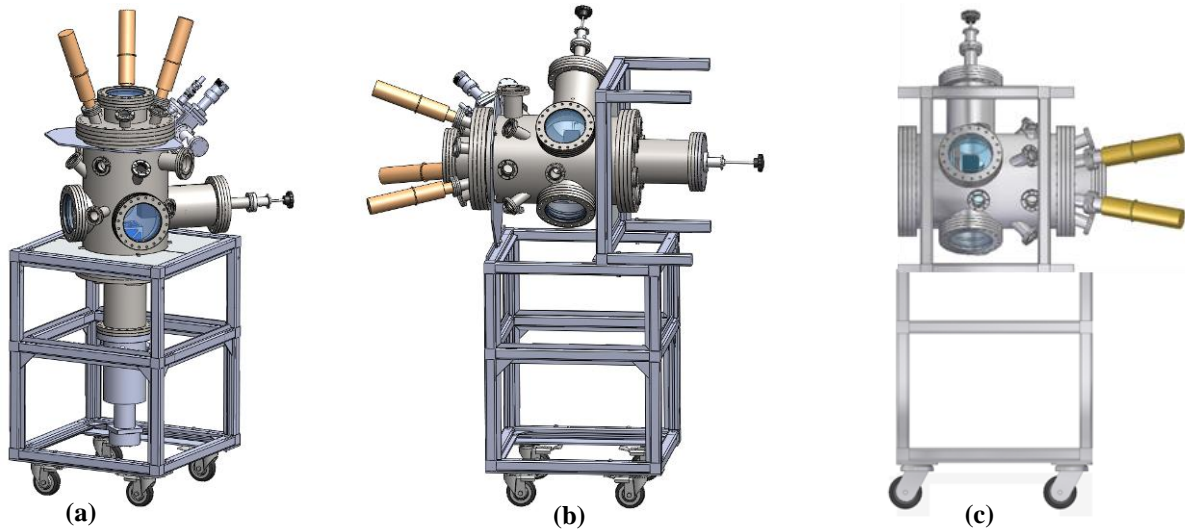


Fig. 4. Space Survivability Test chamber configurations. (a) Vertical configuration. (b) Horizontal configuration. (c) Source flange configuration for mating with other chambers.

are sealed sources with MgF_2 windows (V), but cannot currently be replaced under vacuum.

Electron Fluxes

The SST chamber uses two custom flood guns to provide broad electron beams, with an estimated <2% intensity variation over the full >10 cm x 10 cm sample area. These sources provide highly reliable beams, with <0.1% variation in energy, that are suitable for long duration exposures required for environmental aging tests. They have >95% uniform flux distribution over the full sample area and are continuously monitored during the sample exposure cycle using a standard Faraday cup mounted on the sample block. The flood guns can produce current densities orders of magnitude large than typical space fluxes (see Fig. 1(b)) for accelerated testing.

A low energy electron flood gun (A) provides a uniform, monoenergetic (~20 eV to ~15 keV) flux needed to simulate the solar wind at more than 100X its cumulative electron flux, with electron fluxes at the sample surface of $\leq 5 \cdot 10^6$ electrons- cm^{-2} (~1 pA- cm^{-2} to 1 $\mu A\text{-}cm^{-2}$). The electron gun and control electronics were custom designed at USU after work by Swaminathan.⁴⁵ Beam blanking with a retarding grid is computer controlled and the flux can be manually adjusted during an exposure cycle. The electron gun has dual “hot swappable” filaments for continuous exposure over long duration testing.

The high-energy, low-flux flood gun (~20 keV to ~100 keV) uses photoelectrons produced from a biased metal film on an *in situ* optical substrate. Long-life D_2 lamp

UV sources are mounted exterior to the chamber for easy and rapid bulb replacement. The source is capable of generating very stable low flux beams characteristic of high energy fluxes encountered in space.

Radiation Exposure

A self-contained, portable Sr^{90} beta radiation assembly is shown in Figure 5. Mounting of this source on the SST chamber is shown in Figure 2(a). Previous researchers^{39,46} have identified Sr^{90} beta emission sources as a convenient option for safely emulating the high energy electron radiation environment and testing the effects of electron displacement damage on devices and materials. The small, commercially available 100 mCi encapsulated radiation source mimics high energy (~500 keV to 2.5 MeV) geostationary electron flux (see Figure 1(b)). The half life of Sr^{90} is 29 years, which facilitates stable operation with known dose rates that can be derived from initial and periodic source calibration data. The source provides dose rates up to ~5-10X GEO ambient flux for accelerated testing, with <5% variation over the >10x10 cm sample area.

A computer-controlled pneumatic actuator controls the position of source’s C and W shielding materials to expose samples or materials to radiation. A spring returns the shielding material to its safe position, thereby covering the source. The assembly is contained in a stainless steel storage holder and incorporates *in situ* electronic monitoring capabilities. The design allows simultaneous exposure from the other electron and EMS sources under vacuum and temperature control. The apparatus is also compatible with several different stand alone vacuum chambers.

In Situ Characterization Capabilities

A Labview-based automated data acquisition system periodically monitors and records the environmental conditions and flux intensities *in situ* during the sample exposure cycle. Chamber pressure is monitored with Convectron™, ion gauges (Y) and a residual gas analyzer (Z). Temperature is monitored continuously with platinum resistance probes (K), mounted on the sample stage. Light flux is monitored continuously with photodiodes (I) mounted on the sample stage (M) and equipped with filters to separately monitor NIR, VIS, and UV intensities. Electron flux is monitored continuously with a Faraday cup (J) also mounted on the sample stage. Radiation fluxes are monitored with *in situ* diodes as well.

Limited measurements of sample and materials characteristic and calibration standards can also be made *in situ* during the exposure cycle. A probe stage, mounted on a retractable translation device (T) adds the ability to monitor sample photographs, UV/VIS/NIR reflectivity, IR absorptivity/emissivity, and surface voltage over the samples or CubeSat face, *in situ* during the sample exposure cycle. The sample stage can be rotated to position different samples under the probes. Photographs are made with an external SLR camera by positioning an *in situ* mirror adjacent to a sample. Surface voltage measurements are taken using a modified version of a surface voltage probe apparatus described by Hodges.⁴⁷

Reflectivity is measured with a compact 2.5 cm diameter integrating sphere (H) with a fiber optic connection to two optical spectrometers external to the SST chamber. Two calibrated commercial fiber optic spectrometers (StellarNet, Model BLK-C-SR UV-VIS) (StellarNet, Model RW-InGaAs-512) (F) are used to measure diffuse reflectivity of UV/VIS/NIR (200-1080 nm) and NIR (858-1700 nm) ranges with ≤ 1 nm resolution. Light from a deuterium/W-halogen calibrated light source (Ocean Optics, Model LS-1) enters the integrating sphere through one fiber optic connection; reflected light from the sample exits through another fiber optic to the spectrometers. A split-Y custom fiber optic allows use of a single UHV fiber optic vacuum feedthrough. IR emissivity ($4 \mu\text{m}$ to $15 \mu\text{m}$) is measured with a probe (Omega) (G). The integrating sphere and emissivity probe can be extended over the samples with a retractable linear translation stage (T). High and low reflectivity/emissivity calibration standards (Labsphere, SRS-99, SRS-10) (N) are mounted behind the probe translation stage for *in situ* calibration of the probes.

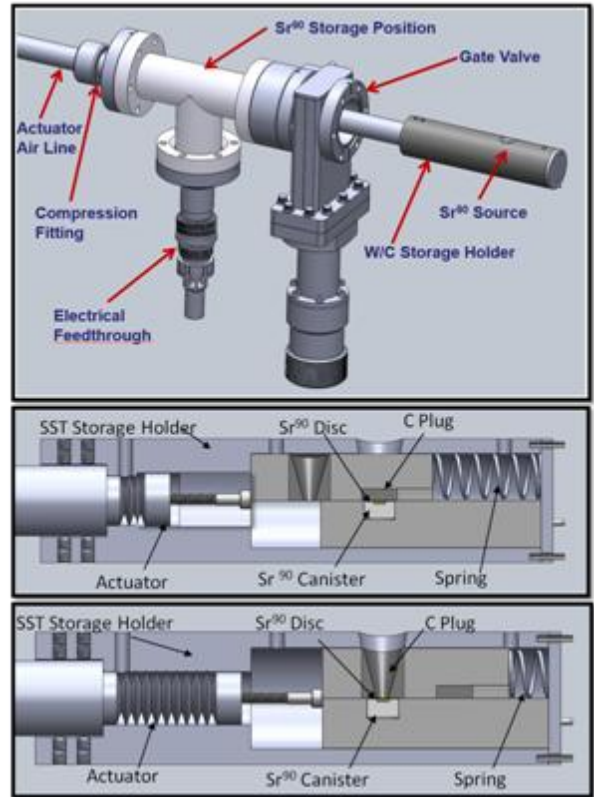


Fig. 5. Sr⁹⁰ radiation source- The 100 mCi encapsulated radiation source emits high energy (~500 keV to 2.5 MeV) electron flux. (a) Exterior detail. Cutaway view with assembly in: (b) closed position, (c) exposure position.

SUMMARY

A versatile test chamber for space survivability studies of small satellites, system components, and materials. The USU Space Survivability Test chamber simulates critical environmental components including the neutral gas atmosphere, temperature, the FUV/UV/VIS/NIR solar spectrum, electron plasma fluxes, and radiation.

Additional work is planned to extend the capabilities of the facility. This includes addition of a low temperature plasma source and an ion beam, a Co⁶⁰ gamma radiation source. Addition of scattering foils to develop broadband electron distributions from the intermediate energy electron gun are being considered.³⁹ There are current plans to include studies of atomic oxygen or high velocity debris impact effects.

Acknowledgments

Funding for this project has been provided by the USU Materials Physics Group and a USU Space Dynamics Laboratory Enabling Technologies Program IR&D Award. We gratefully acknowledge help with the

project from Ethan Lindstrom, Ryan Hoffmann, Joshua Hodges, and Alex Souvall.

References

1. D. Adams, *Hitchhiker's Guide to the Galaxy*, (Del Rey, New York, 1996).
2. D. Hastings, and H. Garrett, *Spacecraft-environment Interactions*, Cambridge University Press, 1996.
3. Shu T. Lai, "Fundamentals of Spacecraft Charging: Spacecraft Interactions with Space Plasmas," Princeton University Press, 2011.
4. K.L. Bedingfield, R.D. Leach and M.B. Alexander, "Spacecraft System Failures and Anomalies Attributed to the Natural Space Environment." NASA Ref. Pub. 1390, NASA MSFC, 1996.
5. R. Leach, and M. Alexander, "Failures and anomalies attributed to spacecraft charging," NASA STI/Recon Technical Report N 96, 11547 (1995).
6. NASA Technical Handbook, "Mitigating In-Space Charging Effects—A Guideline," NASA-STD-4002A, 2011.
7. R. H. Czichy, "Optical design and technologies for space instrumentation," SPIE, vol. 2210, pp. 420-433, April 1994.
8. K. Peterson and J.R. Dennison, "Simulation of UV Radiation Degradation of Polymers on MISSE-6 in the Low Earth Orbit Environment," Utah State Univ. Student Showcase, Logan, UT, April 2, 2013.
9. A. Holmes-Siedle and L. Adams, *Handbook of radiation effects*, 2nd ed., Oxford University Press, pp. 397, 2002. E flux
10. J.R. Srour and J.M. McGarrity, "Radiation effects on microelectronics in space," Proc. IEEE, Vol. 76, No. 11, 1443-1469) 1988.
11. J.R. Dennison, C.D. Thomson, and Alec Sim, "The effect of low energy electron and UV/VIS radiation aging on the electron emission properties and breakdown of thin-film dielectrics," Proc. of the 8th IEEE Dielectrics and Electrical Insulation Soc. (DEIS) International Conf. on Solid Dielectrics (ICSD), Vol. 2, 967-971, (IEEE, Piscataway, NJ, 2004).
12. P. Fortescue, J. Stark and G. Swiner, ed, *Spacecraft Systems Engineering*, 3rd ed., Wiley, pp. 357-361, 2007.
13. R.E. Davies and J.R. Dennison, "Evolution of Secondary Electron Emission Characteristics of Spacecraft Surfaces," *J. Spacecraft and Rockets*, 34, 571-574 (1997).
14. W.Y. Chang, J.R. Dennison, J. Kite and R.E. Davies, "Effects of Evolving Surface Contamination on Spacecraft Charging," Paper AIAA-2000-0868, Proc. of the 38th Am. Inst. of Aeronautics and Astronautics Meeting on Aerospace Sci., (Reno, NV, 2000).
15. A. Evans and J.R. Dennison, "The Effects of Surface Modification on Spacecraft Charging Parameters," *IEEE Trans. on Plasma Sci.*, 40(2), 291-297 (2012).
16. S.T. Lai. "Importance of Surface Conditions for Spacecraft Charging", *J. Spacecraft and Rockets*, Vol. 47, No. 4 (2010), pp. 634-638.
17. D. Ferguson, "New Frontiers in Spacecraft Charging," *IEEE Trans. Plasma Sci.*, vol. 40, no. 2, pp. 1-5, Feb. 2012.
18. J.R. Dennison, "The Dynamic Interplay between Spacecraft Charging, Space Environment Interactions and Evolving Materials," 13th Spacecraft Charging Technology Conf., (Pascadena, CA, June, 2014).
19. L.L.C. Franke, N.J. Schuch, O.S.C. Durão, L.L. Costa, E.E. Bürger, R.Z.G. Bohrer, T.R.C. Stekel, "Analysis of possible failures in satellites Cubesats caused by space environment," COSPAR, 2010.
20. K. Woellert, P. Ehrenfreunda, A.J. Riccob, H. Hertzfelda, "Cubesats: Cost-effective science and technology platforms for emerging and developing nations," *Advances in Space Research* 47 (2011) 663–684.
21. E.G. Lightsey, "Operational Considerations for CubeSats Beyond Low Earth Orbit Beyond Low Earth Orbit," iCubeSat Workshop, Cambridge, MA, May 29, 2012.
22. CubeStat, "NASA Goddard helps expand CubeSats into deep space and 'beyond low earth orbit'," *NASA Goddard Tech Transfer News*, vol. 11, no. 2, p. 5-6, spring 2013
23. S.T. Lai, "Overview of surface and deep dielectric charging on spacecraft," in Shu T Lai, *Spacecraft Charging, Progress in Astronautics and Aeronautics*, Reston, VA, 2011.
24. J.R. Dennison, A.R. Frederickson, N.W. Green, C.E. Benson, J. Brunson and P. Swaminathan, "Materials Database of Resistivities of Spacecraft Materials.," Published electronically by NASA

- Space Environments and Effects Program as part of the Charge Collector Knowledgebase 3rd Ed. at <http://see.msfc.nasa.gov/scck/>
25. J.R. Dennison, A.M. Sim, J. Brunson, S. Hart, J. Gillespie, J. Dekany, C. Sim and D. Arnfield, "Engineering Tool for Temperature, Electric Field and Dose Rate Dependence of High Resistivity Spacecraft Materials Paper Number," AIAA-2009-0562, Proc. of the 47th Am. Inst. of Aeronautics and Astronautics Meeting on Aerospace Sci., 2009.
 26. J.R. Dennison, C.D. Thomson, J. Kite, V. Zavyalov and, J. Corbridge, "Materials Characterization at Utah State University: Facilities and Knowledgebase of Electronic Properties of Materials Applicable to Spacecraft Charging," Proc. of the 8th Spacecraft Charging Techn. Conf., (NASA Marshall Space Flight Center, Huntsville, Al, October 2003), 15 pp.
 27. W.Y. Chang, N. Nickles, J.R. Dennison and C.D. Thomson, "An Improved Database of Electronic Properties of Spacecraft Materials for Modeling of Spacecraft Charging," 7th Spacecraft Charging Techn. Conf., 23-27 April 2000, Noordwijk, The Netherlands.
 28. J.R. Dennison, J. Prebola, A. Evans, D. Fullmer, J.L. Hodges, D.H. Crider and D.S. Crews, "Comparison of Flight and Ground Tests of Environmental Degradation of MISSE-6 SUSpECS Materials," Proc. of the 11th Spacecraft Charging Techn. Conf., (Albuquerque, NM, September, 2010).
 29. J.L. Prebola, , D.H. Crider, , D.S. Crews, "Evaluation of Enhancements to the AEDC Combined Space Environment Chamber", Proc. of 45th AIAA Aerospace Sci. Meeting, Reno, NV, January 2007, Paper AIAA-2007-0092.
 30. T. Paulmier, "SPIDER : A New Test Facility For Charge And Ageing Long-Term Relaxation Analysis, Proc. of the 12th Spacecraft Charging Techn. Conf., (Kitakyushu, Japan, May 14-18, 2012).
 31. R.H. Johnson, L.D. Montierth, J.R. Dennison, J.S. Dyer, and E. Lindstrom, "Small Scale Simulation Chamber for Space Environment Survivability Testing," IEEE Trans. on Plasma Sci., 41(12), 2013, 3453-3458.
 32. W.Y. Chang, J.R. Dennison, N. Nickles and R.E. Davies, "Utah State University Ground-based Test Facility for Study of Electronic Properties of Spacecraft Materials," Proc. 6th Spacecraft Charging Techn. Conf., (AFRL Sci. Center, Hanscom Air Force Base, MA, 2000).
 33. JR Dennison, R.C. Hoffmann, and J. Abbott, "Triggering Threshold Spacecraft Charging with Changes in Electron Emission from Materials," Paper AIAA-2007-1098, Proc. of the 45th Am. Inst. of Aeronautics and Astronautics Meeting on Aerospace Sci., Reno, NV, Jan., 2007.
 34. Grard, J. L. Rejean, "Properties of the Satellite Photoelectron Sheath Derived from Photoemission Laboratory Measurements," J. Geophys. Res., 78(16), 2885, 1973.
 35. B. Feuerbacher and B. Fitton, "Experimental Investigation of Photoemission from Satellite Surface Materials," J. Appl. Phys. 41 1536 (1972).
 36. S.T. Lai, and M. Tautz, "Aspects of Spacecraft Charging in Sunlight," IEEE Tran. on Plasma Sci., Vol. 34, No. 5, October, 2006, pp. 2053-2061.
 37. T. B. Frooninckx, and J.J. Sojka (1992), Solar Cycle Dependence of Spacecraft Charging in Low Earth Orbit, J. Geophys. Res., 97(A3), 2985–2996.
 38. D.J. Rodgers and J. Sørensen, "Internal Charging," in Shu T Lai, Spacecraft Charging, Progress in Astronautics and Aeronautics Reston, VA, 2011.
 39. B. Dirassen, L. Levy, R. Reulet, and D. Payan, "The SIRENE facility - an improved method for simulating the charge of dielectrics in a charging electron environment," Proc. 9th Intern. Symp. Materials in a Space Environment, (June 2003, Noordwijk), ESA SP-540, p. 351 – 358.
 40. ASTM E490 , 2006, "Standard Solar Constant and Zero Air Mass Solar Spectral Irradiance Tables," ASTM International, West Conshohocken, PA, 2006.
 41. J. Minnow, private communications, 2010.
 42. J.I. Minow, E.M. Willis, and L.N. Parker, "Characteristics of Extreme Auroral Charging Events," Proc. 13th Spacecraft Charging Techn. Conf., (Pasadena, CA, June, 2014).
 43. J.R. Dennison and L.H. Pearson, "Pulse Electro-Acoustic (PEA) Measurements of Embedded Charge Distributions," Proc. SPIE Optics and Photonics Conf., Vol. 8876, 2013, pp. 887612-1-887612-11.
 44. J. Dekany, R.H. Johnson, G. Wilson, A. Evans and J.R. Dennison, "Ultrahigh Vacuum Cryostat System for Extended Low Temperature Space

- Environment Testing,” Proc. 12th Spacecraft Charging Techn. Conf., (Kitakyushu, Japan, May, 2012).
45. P.V. Swaminathan, “Measurements of Charge Storage Decay Time and Resistivity of Spacecraft Insulators,” Masters Thesis, Utah State University, Logan, UT 2004.
 46. K. G. Balmain, and W.Hirt, “Dielectric surface discharges - Effects of combined low-energy and high-energy incident electrons,” IEEE Transactions on Electrical Insulation, vol. EI-18, Oct. 1983, p. 498-503.
 47. J.L. Hodges, A.M. Sim, J. Dekany, G. Wilson, A. Evans, and JR Dennison “*In Situ* Surface Voltage Measurements of Layered Dielectrics,” IEEE Trans. on Plasma Sci., 42(1), 2014, 255-265.